

## Improved Step down Conversion in Interleaved Buck Converter and Low Switching Losses

D.Lakshmi (M.Tech) , S.Zabiullah M.Tech, Dr. Venu gopal. N M.E PhD.,

**ABSTRACT**— This project is presented by a soft-switching techniques interleaved buck converter. And it's having order to guarantee small switching losses and, consequently, a high efficiency, a non-dissipative soft-switching cell with auxiliary commutation circuit is used. But in this topology we expected a large step up voltage, low switching stress, small switching losses, and high efficiency.

Because of that we proposed IBC that since the voltage stress across all the active switches is half of the input voltage before turn-on or after turn-off when the operating duty is below 50%, the capacitive discharging and switching losses can be reduced considerably. This allows the proposed IBC to have higher efficiency and operate with higher switching frequency. In that additionally, the proposed IBC has a higher step-down conversion ratio and a smaller output current ripple compared with a conventional IBC. The features, operation principles, and relevant analysis results of the proposed IBC are presented in this project. The validity of this study is confirmed by the experimental results of prototype converters with 150–200 V input, 24 V/10 A output.

**Key words**—Buck converter, interleaved, low switching loss.

### I. INTRODUCTION

A basic buck converter converts a DC voltage to a step down DC voltage. Interleaving adds additional benefits such as reduced ripple currents in both the input and output circuits. Higher efficiency is realized by splitting the output current into two paths, substantially reducing losses and inductor AC losses. In the field of power electronics, application of interleaving technique can be traced back to very early days, especially in high power applications. In high power applications, the voltage and current stress can easily go beyond the range that one power device can handle. Multiple power devices connected in parallel and/or series could be one solution. However, voltage sharing and/or current sharing are still the concerns. Instead of paralleling power devices, paralleling power converters is another solution which could be more beneficial. Benefits like harmonic cancellation, better efficiency, better thermal performance, and high power density.

An interleaved buck converter usually combines more than two conventional topologies, and the current in the element of the interleaved buck converter is half of the conventional topology in the same power condition. The single buck converter can use the zero-voltage switching (ZVS) and/or zero-current switching (ZCS) to reduce the switching loss of the high-frequency switching. However, they are considered for the single topology.

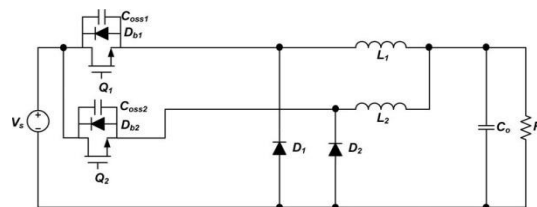


Fig (1) conventional IBC

In Applications where nonisolation, step-down conversion ratio, and high output current with low ripple are required, an interleaved buck converter (IBC) has received a lot of attention due to its simple structure and low control complexity. However, in the conventional IBC shown in Fig. 1, all semiconductor devices suffer from the input voltage, and hence, high-voltage devices rated above the input voltage should be used. High-voltage-rated devices have generally poor characteristics such as high cost, high on-resistance, high forward voltage drop, severe reverse recovery, etc. In addition, the converter operates under hard switching condition. Thus, the cost becomes high and the efficiency becomes poor. And, for higher power density and better dynamics, it is required that the converter operates at higher switching frequencies. However, higher switching frequencies increase the switching losses associated with turn-on, turn-off, and reverse recovery. Consequently, the efficiency is further deteriorated. Also, it experiences an extremely short duty cycle in the case of high-input and low-output voltage applications.

In previous applications, the PWM control is used in the converter circuits to get the desired shape of the output voltage or current. By using this technique the following disadvantages are occurs:

1. The devices are turned on and off at the load current with a high di/dt value
  2. The switches are subjected to a high-voltage stress.
  3. The switching power loss also increases with the switching frequency.
  4. The turn on and turn off loss could be a significant portion of the total power loss.
  5. The electromagnetic interference is also produced due to high di/dt and du/dt in the converter waveforms.
- The above disadvantages can be eliminated (or) minimized if the devices are turned ‘ON’ and ‘OFF’ by using soft switching technique. These are Zero Voltage Switching and Zero Current Switching.

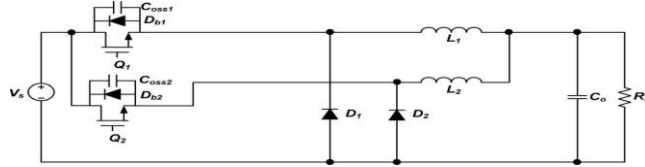


Fig (2) proposed IBC

The new IBC, which is suitable for the applications where the input voltage is high and the operating duty is below 50%, is proposed. It is similar to the conventional IBC, but two active switches are connected in series and a coupling capacitor is employed in the power path. The two active switches are driven with the phase shift angle of 180° and the output voltage is regulated by adjusting the duty cycle at a fixed switching frequency. The features of the proposed IBC are similar to those of the IBC in [14]. Since the proposed IBC also operates at CCM, the current stress is low. During the steady state, the voltage stress across all active switches before turn-on or after turn-off is half of the input voltage. Thus, the capacitive discharging and switching losses can be reduced considerably. The voltage stress of the freewheeling diodes is also lower than that of the conventional IBC so that the reverse-recovery and conduction losses on the freewheeling diodes can be improved by employing schottky diodes that have generally low breakdown voltages, typically below 200 V. The conversion ratio and output current ripple are lower than those of the conventional IBC.

## II. CIRCUIT OPERATIONS

Fig. 2 shows the circuit configuration of the proposed IBC. The structure is similar to a conventional IBC except two active switches in series and a coupling capacitor employed in the power path. Figs. 3 and 6 show the key operating waveforms of the proposed IBC in the steady state. Referring to the figures, it can be seen that switches  $Q_1$  and  $Q_2$  are driven with the phase shift angle of 180°. This is the same as that for a conventional IBC. Each switching period is divided into four modes, whose operating circuits are shown in Figs. 4 and 5. In order to illustrate the operation of the proposed IBC, some assumptions are made as follows:

- 1) the output capacitor  $C_O$  is large enough to be considered as a voltage source;
- 2) the two inductors  $L_1$  and  $L_2$  have the same inductance  $L$ ;
- 3) all power semiconductors are ideal;
- 4) the coupling capacitor  $C_B$  is large enough to be considered as a voltage source.

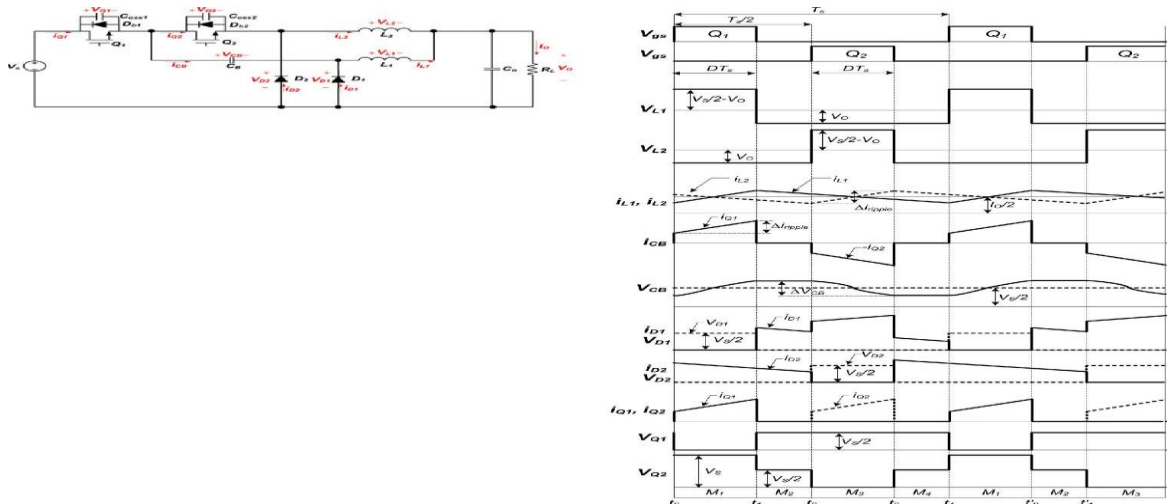


Fig. 3. Key operating waveforms of the proposed IBC when  $D \leq 0.5$ .

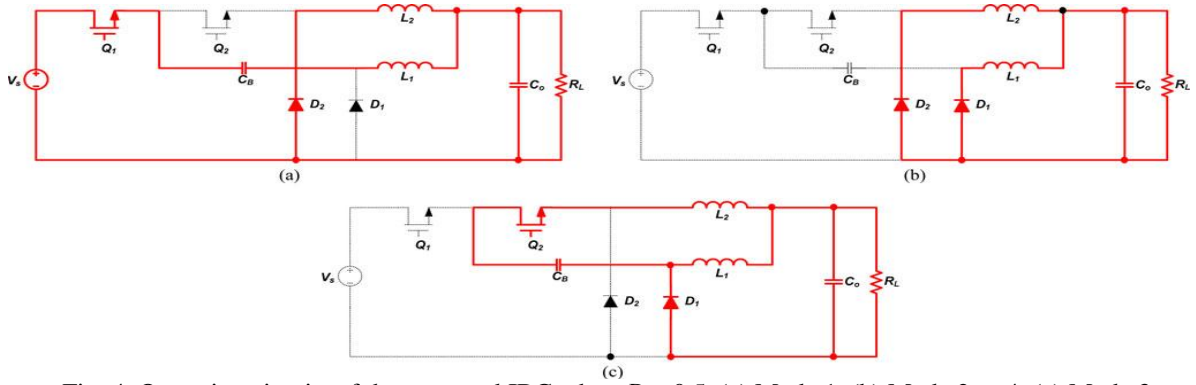


Fig. 4. Operating circuits of the proposed IBC when  $D \leq 0.5$ . (a) Mode 1. (b) Mode 2 or 4. (c) Mode 3.

### A. Steady-State Operation when $D \leq 0.5$

Mode 1 [ $t_0 - t_1$ ]: Mode 1 begins when  $Q_1$  is turned ON at  $t_0$ . Then, the current of  $L_1$ ,  $i_{L1}(t)$ , flows through  $Q_1$ ,  $C_B$ , and  $L_1$  and the voltage of the coupling capacitor  $V_{CB}$  is charged. The current of  $L_2$ ,  $i_{L2}(t)$ , freewheels through  $D_2$ . During this mode, the voltage across  $L_1$ ,  $V_{L1}(t)$ , is the difference of the input voltage  $V_S$ , the voltage of the coupling capacitor  $V_{CB}$ , and the output voltage  $V_O$ , and its level is positive. Hence,  $i_{L1}(t)$  increases linearly from the initial value. The voltage across  $L_2$ ,  $V_{L2}(t)$ , is the negative output voltage, and hence,  $i_{L2}(t)$  decreases linearly from the initial value. The voltage across  $Q_2$ ,  $V_{Q2}(t)$ , becomes the input voltage and the voltage across  $D_1$ ,  $V_{D1}(t)$ , is equal to the difference of  $V_S$  and  $V_{CB}$ . The voltages and currents can be expressed as follows:

$$V_{L1}(t) = V_S - V_{CB} - V_O \quad (1)$$

$$V_{L2}(t) = -V_O \quad (2)$$

$$i_{L1}(t) = V_S - V_{CB} - V_O / L(t - t_0) + i_{L1}(t_0) \\ = i_{Q1}(t) = i_{CB}(t) \quad (3)$$

$$i_{L2}(t) = -V_O / L(t - t_0) + i_{L2}(t_0) = i_{D2}(t) \quad (4)$$

$$V_{Q2} = V_S \quad (5)$$

$$V_{D1} = V_S - V_{CB} \quad (6)$$

$$V_{CB} = V_{CB}(t_0) + I_O / 2C_B(t - t_0) \quad (7)$$

Mode 2 [ $t_1 - t_2$ ]: Mode 2 begins when  $Q_1$  is turned OFF at  $t_1$ . Then,  $i_{L1}(t)$  and  $i_{L2}(t)$  freewheel through  $D_1$  and  $D_2$ , respectively. Both  $V_{L1}(t)$  and  $V_{L2}(t)$  become the negative  $V_O$ , and hence,  $i_{L1}(t)$  and  $i_{L2}(t)$  decrease linearly. During this mode, the voltage across  $Q_1$ ,  $V_{Q1}(t)$ , is equal to the difference of  $V_S$  and  $V_{CB}$  and  $V_{Q2}(t)$  becomes  $V_{CB}$ . The voltages and currents can be expressed as follows:

$$V_{L1}(t) = V_{L2}(t) = -V_O \quad (8)$$

$$i_{L1}(t) = i_{L1}(t_1) - (V_O / L)(t - t_1) = i_{D1}(t) \quad (9)$$

$$i_{L2}(t) = i_{L2}(t_1) - (V_O / L)(t - t_1) = i_{D2}(t) \quad (10)$$

$$V_{Q1}(t) = V_S - V_{CB} \quad (11)$$

$$V_{Q2}(t) = V_{CB} \quad (12)$$

Mode 3 [ $t_2 - t_3$ ]: Mode 3 begins when  $Q_2$  is turned ON at  $t_2$ . At the same time,  $D_2$  is turned OFF. Then,  $i_{L1}(t)$  freewheels through  $D_1$  and  $i_{L2}(t)$  flows through  $D_1$ ,  $C_B$ ,  $Q_2$ , and  $L_2$ . Thus,  $V_{CB}$  is discharged. During this mode,  $V_{L2}(t)$  is equal to the difference of  $V_{CB}$  and  $V_O$  and its level is positive. Hence,  $i_{L2}(t)$  increases linearly.  $V_{L1}(t)$  is the negative  $V_O$ , and hence,  $i_{L1}(t)$  decreases linearly. The voltages and currents can be expressed as follows:

$$V_{L1}(t) = -V_O \quad (13)$$

$$V_{L2}(t) = V_{CB} - V_O \quad (14)$$

$$i_{L1}(t) = (-V_O / L)(t - t_2) + i_{L1}(t_2) \quad (15)$$

$$i_{L2}(t) = (V_{CB} - V_O) / L(t - t_2) + i_{L2}(t_2) \quad (16)$$

$$= i_{Q2}(t) = -i_{CB}(t) \quad (17)$$

$$i_{D1}(t) = i_{L1}(t) + i_{L2}(t) \quad (18)$$

$$V_{Q1} = V_S - V_{CB} \quad (19)$$

$$V_{D2} = V_{CB} \quad (20)$$

$$V_{CB} = V_{CB}(t_2) - (I_O / 2C_B)(t - t_2) \quad (20)$$

Mode 4 [ $t_3 - t_4$ ]: Mode 4 begins when  $Q_2$  is turned OFF at  $t_3$ , and its operation is the same with that of mode 2.

The steady-state operation of the proposed IBC operating with the duty cycle of  $D \leq 0.5$  has been described. From the operation principles, it is known that the voltage stress of all semiconductor devices except  $Q2$  is not the input voltage, but is determined by the voltage of coupling capacitor  $VCB$ . The maximum voltage of  $Q2$  is the input voltage, but the voltage before turn-on or after turn-off is equal to  $VCB$ . As these results, the capacitive discharging and switching losses on  $Q1$  and  $Q2$  can be reduced considerably. In addition, since diodes with good characteristics such as schottky can be used for  $D1$  and  $D2$ , the reverse-recovery and conduction losses can be also improved. The loss analysis will be discussed in detail in the next section.

### B. Steady-State Operation When $D > 0.5$

Mode 1 [ $t_0 - t_1$ ]: Mode 1 begins when  $Q2$  is in on-state and  $Q1$  is turned ON at  $t_0$ . Then,  $iL1(t)$  flows through  $Q1$ ,  $CB$ , and  $L1$  and  $VCB(t)$  is charged.  $iL2(t)$  flows through  $Q1$ ,  $Q2$ , and  $L2$ .  $VL1(t)$  is equal to the difference of  $VS$ ,  $VCB$ , and  $VO$  and its level is positive. Thus,  $iL1(t)$  increases linearly from the initial value.  $VL2(t)$  is equal to the difference of  $VS$  and  $VO$  and  $iL2(t)$  also increases linearly from the initial value. The voltages and currents can be expressed as follows:

$$VL1(t) = VS - VCB - VO \quad (21)$$

$$VL2(t) = VS - VO \quad (22)$$

$$VD1 = VS - VCB \quad (23)$$

$$VD2 = VS \quad (24)$$

$$iQ1 = iL1(t) + iL2(t) \quad (25)$$

$$iQ2 = iL2(t). \quad (26)$$

Mode 2 [ $t_1 - t_2$ ]: Mode 2 begins when  $Q2$  is turned OFF at  $t_1$ . Then,  $iL1(t)$  flows through  $Q1$ ,  $CB$ , and  $L1$  and  $iL2(t)$  freewheels through  $D2$ . The operation during this mode is the same with mode 1 in the case of  $D \leq 0.5$ .

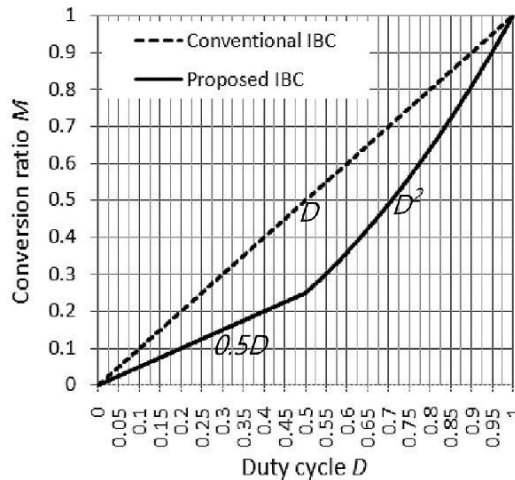
Mode 3 [ $t_2 - t_3$ ]: Mode 3 begins when  $Q2$  is turned ON at  $t_2$ , and the operation is the same with mode 1.

Mode 4 [ $t_3 - t_4$ ]: Mode 4 begins when  $Q1$  is turned OFF at  $t_3$ . Then,  $iL1(t)$  freewheels through  $D1$  and  $iL2(t)$  flows through  $D1$ ,  $CB$ ,  $Q2$ , and  $L2$ . Thus,  $VCB$  is discharged. The operation during this mode is the same with mode 3 in the case of  $D \leq 0.5$ .

The steady-state operation of the proposed IBC operating with  $D > 0.5$  has been described. Under this operating condition, the voltage stress of  $Q1$  and  $D1$  is determined by  $VCB$ , but the voltage stress of  $Q2$  and  $D2$  is determined by the input voltage. In addition, since  $VL2(t)$  is much larger than  $VL1(t)$  during mode 1 or mode 3, the unbalance between  $iL1(t)$  and  $iL2(t)$  occurs, as shown in Fig. 6. The current of  $Q1$ ,  $iQ1(t)$ , is the sum of  $iL1(t)$  and  $iL2(t)$  and the current of  $Q2$ ,  $iQ2(t)$ , is equal to  $iL2(t)$  in mode 1 or mode 3. Therefore, it can be said that switches  $Q1$  and  $Q2$  experience high current stress in the case of  $D > 0.5$ . Until now, the steady-state operation of the proposed IBC has been described in detail. Consequently, it can be known that the proposed IBC has advantages in terms of efficiency and component stress in the case of only  $D \leq 0.5$ . Thus, the proposed IBC is recommended for the applications where the operating duty cycle is smaller than or equal to 0.5.

### III. RELEVANT ANALYSIS RESULTS

The proposed IBC will be only employed in the applications where the operating duty cycle is below 0.5, but the following relevant analyses are conducted over the entire duty cycle range for a detail design guide.



**DC Conversion Ratio**

The dc conversion ratio of the proposed IBC can be derived using the principle of inductor volt-second-balance (VSB) .In the case of  $D \leq 0.5$ , the following equations can be obtained from the VSB of  $L_1$  and  $L_2$  , respectively

$$(V_S - V_{CB} - V_O)DT_S = V_O(1 - D)T_S \quad (27)$$

$$(V_{CB} - V_O)DT_S = V_O(1 - D)T_S \quad (28)$$

The voltage of the coupling capacitor can be obtained by substituting (28) into (27) and is equal to half of the input voltage as follows:

$$V_{CB} = V_S/2 \quad (29)$$

Then, the dc conversion ratio  $M$  can be obtained from (27) and (29) or (28) and (29) as follows:

$$M = V_O/V_S = D/2 \quad (30)$$

In the case of  $D > 0.5$ , the voltage of the coupling capacitor and the dc conversion ratio can be obtained by the same procedure and are expressed as follows, respectively

$$V_{CB} = V_S(1 - D) \quad (31)$$

The proposed IBC has a higher step-down conversion

As a result, the proposed IBC can overcome the extremely short duty cycle, which appears in the conventional IBC. ratio than the conventional IBC

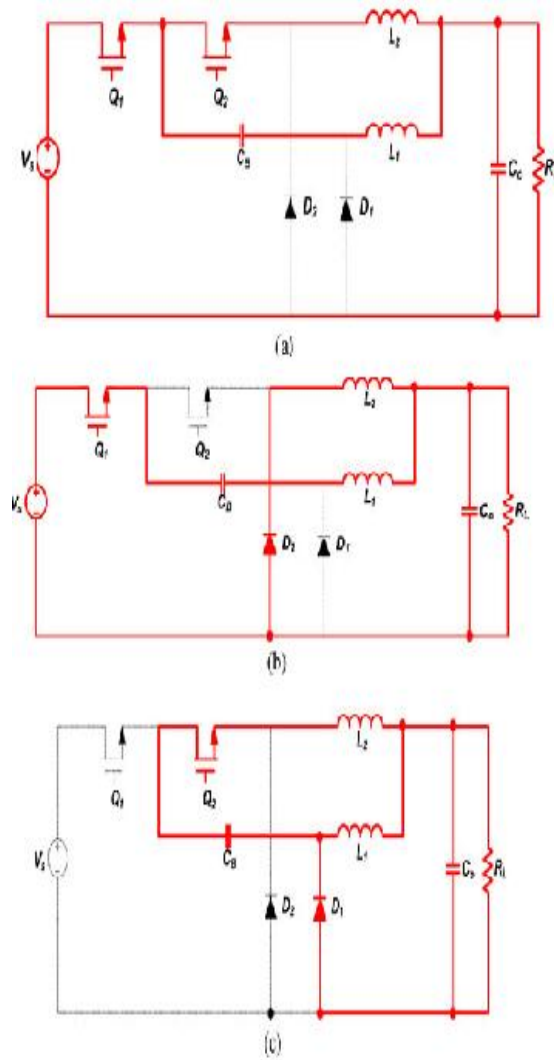


Fig. 5. Operating circuits of the proposed IBC when  $D > 0.5$  (a) Mode1 or 3.(b)Mode2.(c) Mode4.

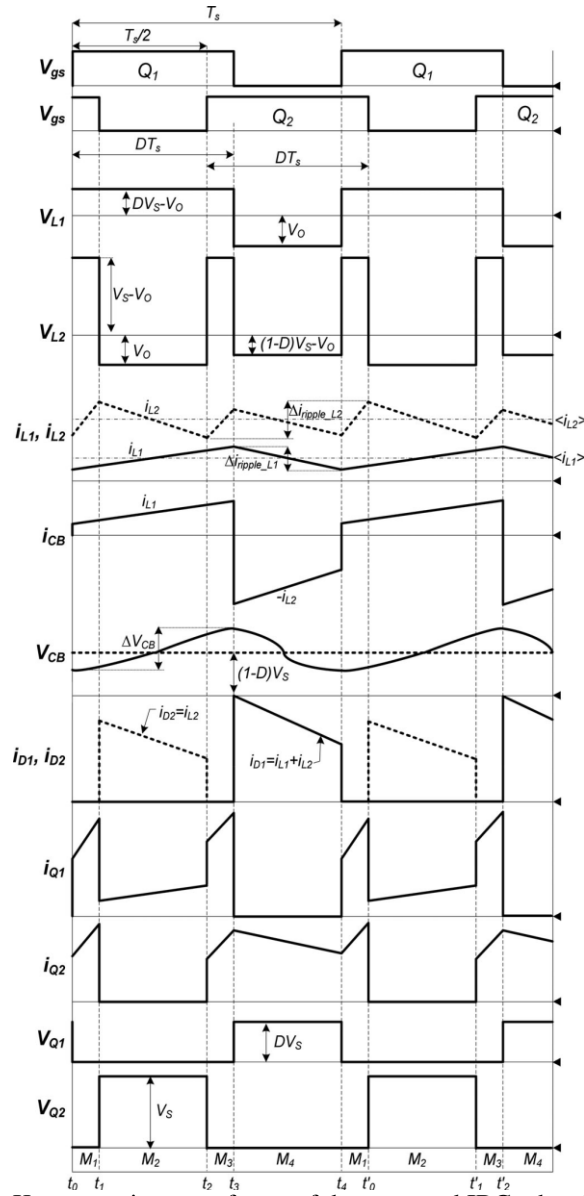


Fig. 6. Key operating waveforms of the proposed IBC when  $D > 0.5$ .

### EXPERIMENTAL RESULTS

The proposed and conventional IBCs are realized with the specifications shown next.

- 1) Input voltage:  $V_S = 150\text{--}200$  V.
- 2) Output voltage:  $V_O = 24$  V.
- 3) Output current:  $I_O = 10$  A.
- 4) Switching frequency:  $f_S = 65$  kHz or 300 kHz.
- 5) Inductor ripple current: below 3 A.
- 6) Ripple voltage of a coupling capacitor: below 4 V.
- 7) Output voltage ripple: below 250 mV.

The prototypes for the experiment, which are the conventional IBC and proposed IBCs, have been built and tested to verify the operational principle, advantages, and performances of the proposed IBC, using the components as shown in Table III. In order to alleviate the ringing caused by parasitic elements, two simple RC snubbers are used across diodes  $D_1$  and  $D_2$ , respectively. Their values are as follows:

$$R = 10 \Omega / W, C = 10 \text{ nF} / 630 \text{ V}.$$

For the experiment of the proposed IBC2, which is the proposed IBC with lower voltage rated freewheeling diodes, the auxiliary circuit described in Section III is added.

III. Simulation circuits and outputs of the proposed IBC from  $D < 50\%$

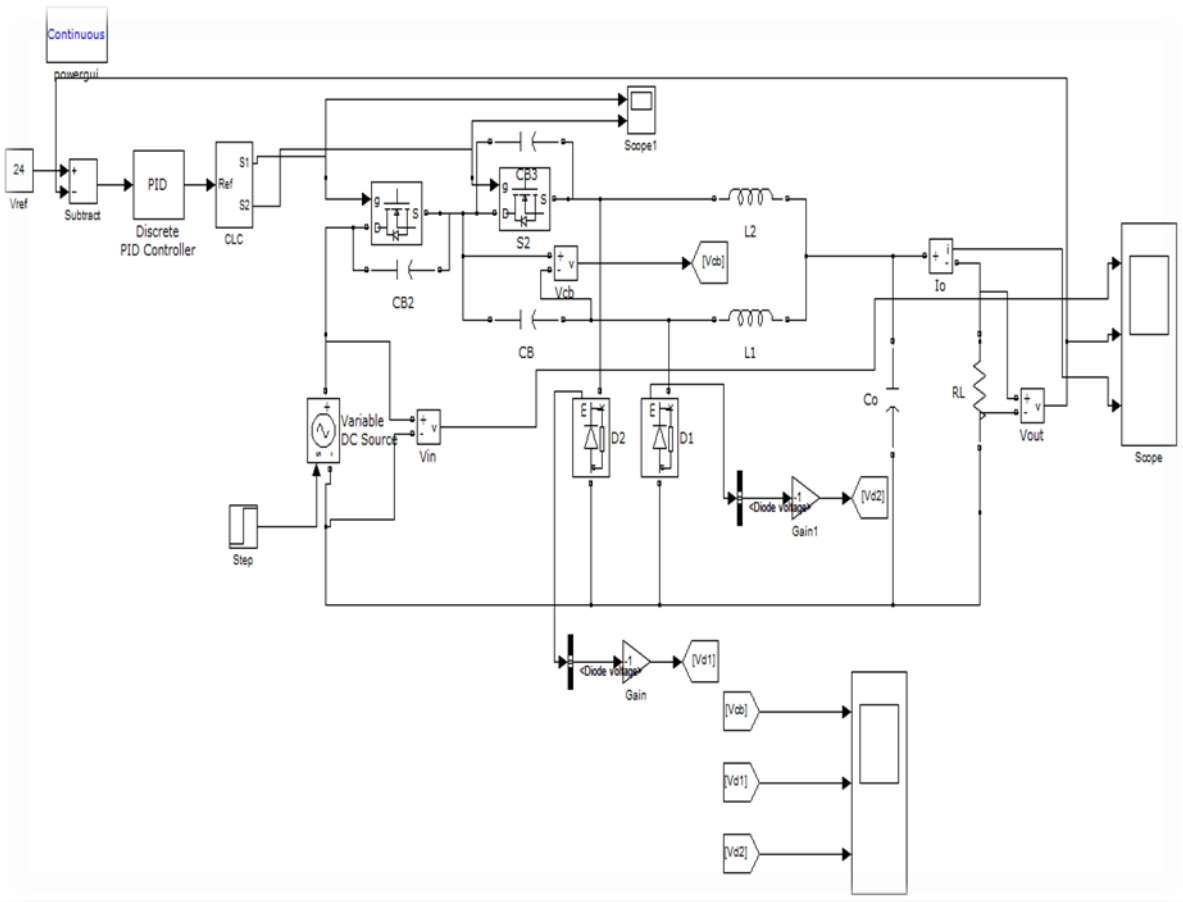
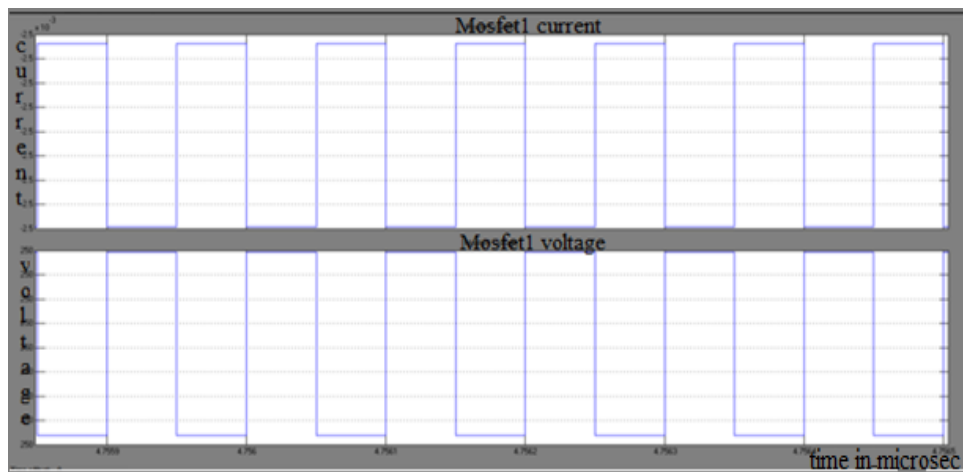
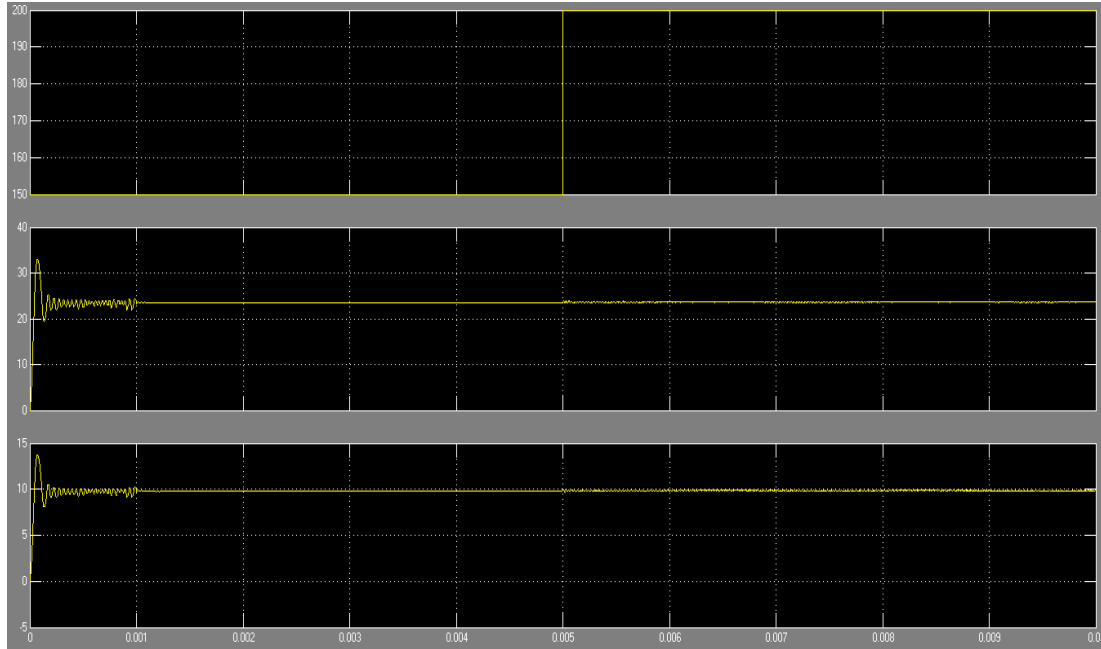


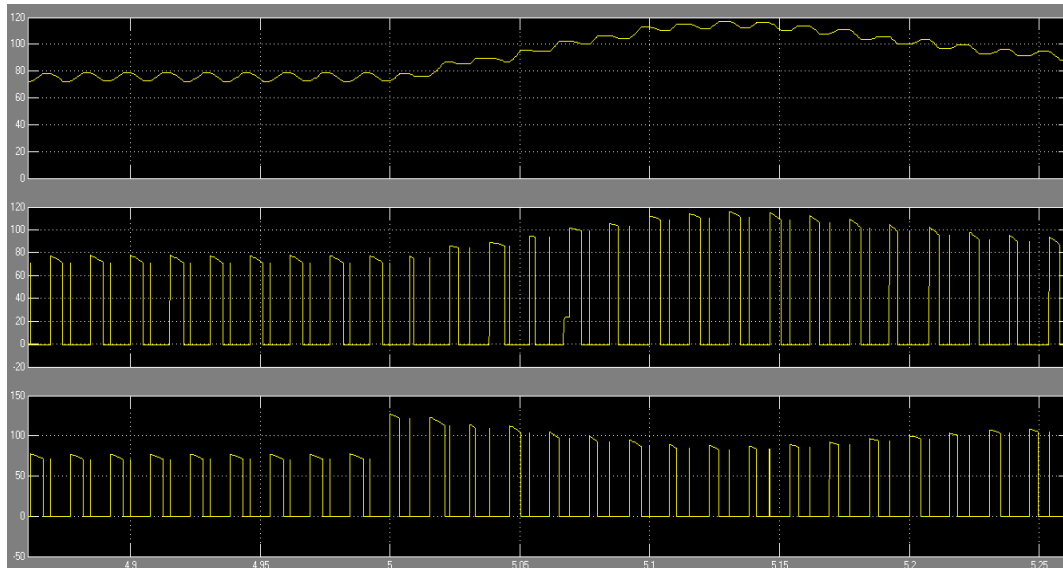
Fig: (7) Simulink Model of R Load Proposed diagram from  $D < 50\%$



Fig(8). Triggering pulses for R-load



Fig(9). Output voltage for proposed R-load



Fig(10). Coupling capacitor voltage wave & Diode 1 voltage& Diode 2 voltage output waveforms For R-Load

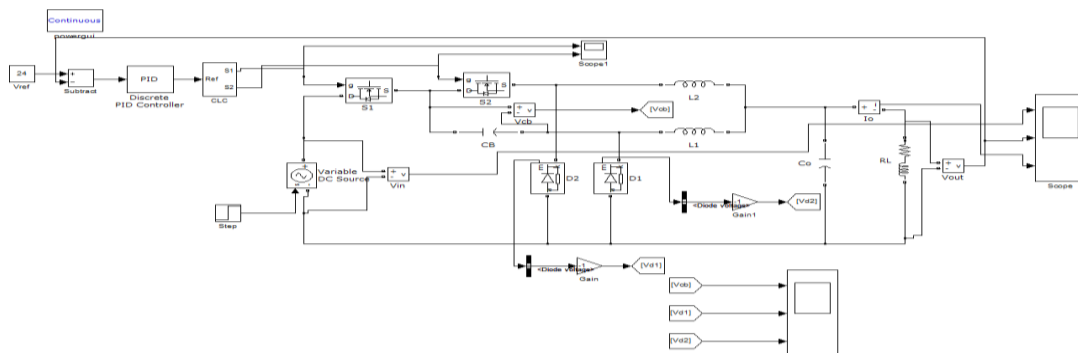
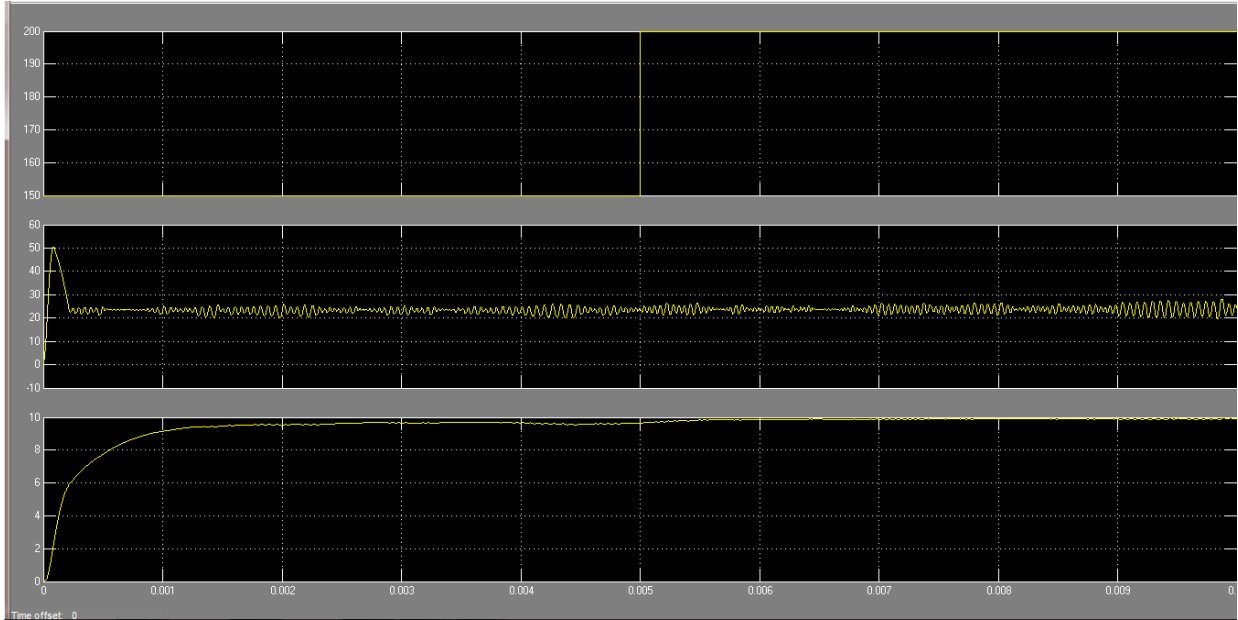
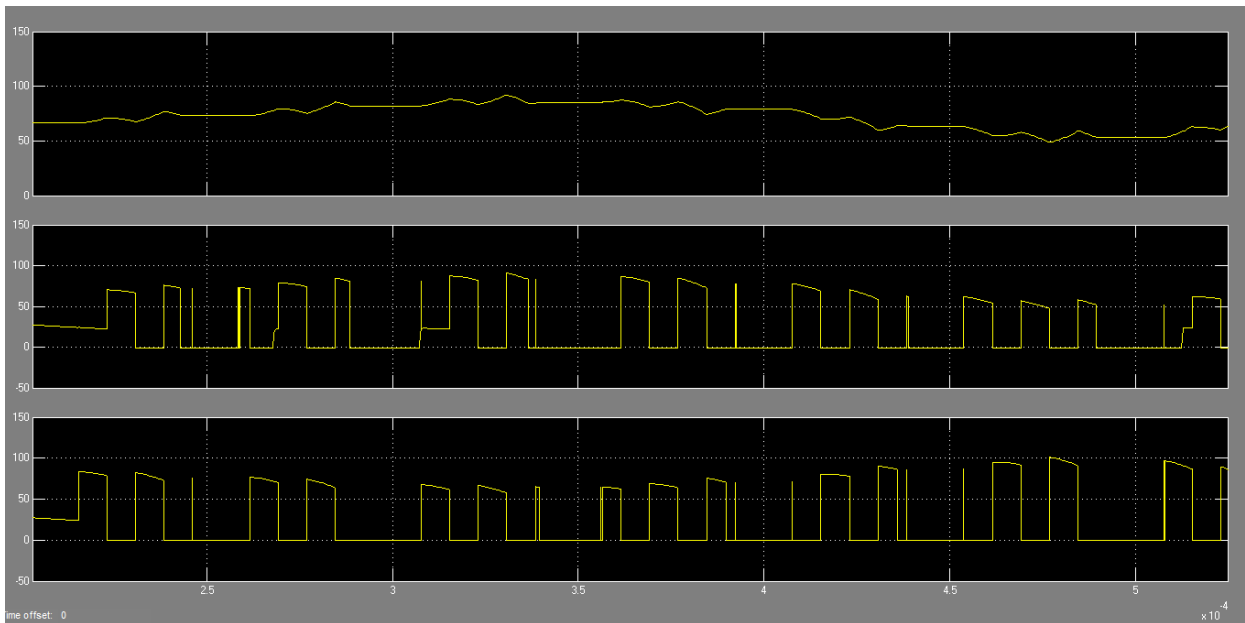


Fig: (11) Simulink Model of RL Load Proposed diagram from  $D < 50\%$  For RL-Load



**Fig(12). Output voltage for proposed RL-load**



**Fig(13). Coupling capacitor voltage wave & Diode 1 voltage& Diode 2 voltage output waveforms For RL-Load**

#### IV. CONCLUSION

A new IBC is proposed in this project. While keeping the good characteristics of the IBC introduced in [14], it has a more simple structure. The main advantage of the proposed IBC is that since the voltage stress across active switches is half of the input voltage before turn-on or after turn-off when the operating duty is below 50%, the capacitive discharging and switching losses can be reduced considerably. In addition, since the voltage stress of the freewheeling diodes is half of the input voltage in the steady state and can be quickly reduced below the input voltage during the cold startup, the use of lower voltage-rated diodes is allowed. Thus, the losses related to the diodes can be improved by employing schottky diodes that have generally low breakdown voltages, typically below 200V. From these results, the efficiency of the proposed IBC is higher than that of the conventional IBC and the improvement gets larger as the switching frequency increases. These are verified with the experimental results. Moreover, it is confirmed that the proposed IBC has a higher step-down conversion ratio and a smaller inductor current ripple than the conventional IBC. Therefore, the proposed IBC becomes attractive in applications where non isolation, step-down conversion ratio with high input voltage, high output current with low ripple, higher power density, and low cost are required.

## REFERENCES

- [1] P. L. Wong, P. Xu, B. Yang, and F. C. Lee, "Performance improvements of interleaving VRMs with coupling inductors," *IEEE Trans. Power Electron.*, vol. 168, no. 4, pp. 499–507, Jul. 2001.
- [2] R. L. Lin, C. C. Hsu, and S. K. Changchien, "Interleaved four-phase buck-based current source with isolated energy-recovery scheme for electrical discharge machine," *IEEE Trans. Power Electron.*, vol. 24, no. 7, pp. 2249–2258, Jul. 2009.
- [3] C. Garcia, P. Zumel, A. D. Castro, and J. A. Cobos, "Automotive DC–DC bidirectional converter made with many interleaved buck stages," *IEEE Trans. Power Electron.*, vol. 21, no. 21, pp. 578–586, May 2006.
- [4] J. H. Lee, H. S. Bae, and B. H. Cho, "Resistive control for a photovoltaic battery charging system using a microcontroller," *IEEE Trans. Ind. Electron.*, vol. 55, no. 7, pp. 2767–2775, Jul. 2008.
- [5] Y. C. Chuang, "High-efficiency ZCS buck converter for rechargeable batteries," *IEEE Trans. Ind. Electron.*, vol. 57, no. 7, pp. 2463–2472, Jul. 2010.
- [6] C. S. Moo, Y. J. Chen, H. L. Cheng, and Y. C. Hsieh, "Twin-buck converter with zero-voltage-transition," *IEEE Trans. Ind. Electron.*, vol. 58, no. 6, pp. 2366–2371, Jun. 2011.
- [7] X. Du and H. M. Tai, "Double-frequency buck converter," *IEEE Trans. Ind. Electron.*, vol. 56, no. 54, pp. 1690–1698, May 2009.
- [8] K. Jin and X. Ruan, "Zero-voltage-switching multiresonant three-level converters," *IEEE Trans. Ind. Electron.*, vol. 54, no. 3, pp. 1705–1715, Jun. 2007.
- [9] J. P. Rodrigues, S. A. Mussa, M. L. Heldwein, and A. J. Perin, "Three level ZVS active clamping PWM for the DC–DC buck converter," *IEEE Trans. Power Electron.*, vol. 24, no. 10, pp. 2249–2258, Oct. 2009.
- [10] X. Ruan, B. Li, Q. Chen, S. C. Tan, and C. K. Tse, "Fundamental considerations of three-level DC–DC converters: Topologies, analysis, and control," *IEEE Trans. Circuit Syst.*, vol. 55, no. 11, pp. 3733–3743, Dec. 2008.
- [11] Y. M. Chen, S. Y. Teseng, C. T. Tsai, and T. F. Wu, "Interleaved buck converters with a single-capacitor turn-off snubber," *IEEE Trans. Aerosp. Electronic Syst.*, vol. 40, no. 3, pp. 954–967, Jul. 2004.
- [12] C. T. Tsai and C. L. Shen, "Interleaved soft-switching coupled-buck converter with active-clamp circuits," in *Proc. IEEE Int. Conf. Power Electron. and Drive Systems.*, 2009, pp. 1113–1118.
- [13] M. Ilic and D. Maksimovic, "Interleaved zero-current-transition buck converter," *IEEE Trans. Ind. App.*, vol. 43, no. 6, pp. 1619–1627, Nov. 2007.
- [14] K. Yao, Y. Qiu, M. Xu, and F. C. Lee, "A novel winding-coupled buck converter for high-frequency, high-step-down DC–DC conversion," *IEEE Trans. Power Electron.*, vol. 20, no. 5, pp. 1017–1023, Sep. 2005.



**D. Lakshmi** <sup>M.Tech</sup> Student from Kuppam Engineering College at Kuppam (JNTUA). I was awarded B.Tech from Kuppam Engineering College at Kuppam (JNTU A) in 2011.



**S. Zabiullah** <sup>M.Tech.</sup> working as Assistant Professor, he was awarded M.Tech from Sri Venkateshwara College of Engineering & Technologies in Chittoor (JNTU A) in 2011, he was awarded B.Tech from (JNTU A) in 2009. He has 3 years of teaching experience. His area of interest is Power Electronics & Electrical Drives.



**Dr. Venugopal** <sup>ME, Ph.D.</sup>, working as Professor, he was awarded Ph.D (video processing) from Dr. MGR University, Chennai, in 2011, he was awarded M.E (Power electronics) from University Visveshwaraya College of Engineering, Bangalore, in 1998, he was awarded B.E (EEE) from R.V. College of Engineering, Bangalore, in 1995. He has 16 years of teaching experience and he is currently working as Director (Research & Development) in Kuppam engineering college, kuppam. His research area interested in power electronics, video processing, power systems & renewable energy sources.